



X International Conference on Structural Dynamics, EURODYN 2017

Vibration mitigation of a linear host structure using a passive neutralizer: effect of nonlinearity in the neutralizer suspension

R. Aiello^a, G. Gatti^{a*}

^aDepartment of Mechanical, Energy and Management Engineering, University of Calabria, Arcavacata di Rente (CS) 87036, Italy

Abstract

Motivated by some experimental results on a test-rig, this paper presents some observations on the frequency response of a primary linear oscillator when an auxiliary nonlinear oscillator is attached to it, acting as a vibration neutralizer. In the experiments, an electro-dynamic shaker is used as the linear one-degree-of-freedom primary oscillator, and it is excited by an harmonic force. The nonlinear neutralizer is attached to the moving head of the shaker, and it is assembled to achieve a cubic stiffness characteristics, due to geometrical arrangement of linear elastic elements. For very low vibration amplitudes, the whole system behaves predominantly as a two-degree-of-freedom linear oscillator, but when the force excitation to the shaker is increased the shape of the frequency response curve changes, and exhibits resonance peak bending, jump phenomena and instabilities of the harmonic response. A theoretical model of the system is presented, with the aim to capture the qualitative phenomena observed in the experiments.

© 2017 The Authors. Published by Elsevier Ltd.

Peer-review under responsibility of the organizing committee of EURODYN 2017.

Keywords: Vibration neutraliser; nonlinear vibration; mass damper

1. Introduction

A vibration neutralizer basically consists of an auxiliary mass attached to a vibrating host structure through a suspension system, with proper stiffness and damping elements, for vibration mitigation purposes. The first vibration neutralizer was patented by Frahm [1] and then theoretically investigated in [2]. Following these pioneering studies, several works have been conducted, and focus was devoted to the practical implementations [3-5].

* Corresponding author. Tel.: +39-0984-494157; fax: +39-0984-494673.

E-mail address: gianluca.gatti@unical.it

For a light-damped linear case, the frequency response curve (FRC) of the primary mass displacement presents an anti-resonance at a frequency equal to the natural frequency of the neutralizer alone. This feature is exploited to reduce the vibration amplitude of the host structure, by tuning the neutralizer natural frequency to the excitation frequency to which the host structure is subject. However, the introduction of the anti-resonance is complemented by the introduction of a further resonance peak, and this could be one major drawback, since it can potentially increase the vibration of the host structure if the forcing frequency changes. To overcome this problem, with a linear system, one could increase the mass of the neutralizer, but this is often undesirable [5].

This paper builds on experimental observations of the dynamics of a nonlinear oscillator attached to an electro-dynamic shaker, and presents a theoretical model to qualitatively capture the fundamental phenomena.

2. Experimental observation

The test-rig considered in this work, and the corresponding experimental setup, is presented in Fig. 1(a) and (b), respectively. The test-rig consists of an electro-dynamic shaker, on the moving head of which a support structure is attached. The shaker is tilted so that its vibration is on the horizontal axis. The total mass of the primary system thus consists of the moving mass of the shaker plus the mass of the attached support structure. This latter is exploited to hold the oscillating mass of the neutralizer, which consists of a plastic bolt with a few metal nuts suspended by nylon wires. The mass of the attachment is much smaller than the mass of the primary system, and due to the geometric arrangement of the wires and their symmetry, it is constrained to move primarily in the horizontal direction. Two accelerometers are used to measure the motion of the two masses, and they are indicated in Fig. 1(a) as well. The accelerometers are connected to a frequency analyser, controlled by a PC, as shown in Fig. 1(b). The shaker is excited by a signal generator through a power amplifier. A current meter is used to measure the current flowing in the shaker coil. All the main items of equipment are indicated in the photograph of Fig. 1(b).

In a preliminary phase, experimental tests were performed by supplying a low-level white noise signal to the shaker. The current supply and the accelerations of both masses were measured, and the FRC was estimated, which is presented in terms of displacement amplitude per unit current. Two specific cases were considered: in the first case, the tension in the wires was adjusted so that it was tighter than in the second case. This was achieved by manually tightening/loosening wires upon assembly.

Experimental results for low-level excitation are shown in Fig. 2(a-d) as blue solid lines. In particular, Fig. 2(a) and (b) show the amplitude of the displacement of the primary mass and the attachment, respectively, per unit current, in the case of tighter wires. Figure 2(c) and (d) show the amplitude of the displacement of the primary mass and the attachment, respectively, per unit current, in the case of looser wires.

From Figs. 2(a) and (c) it can be clearly seen the effect of the neutralizer on the primary mass, which is to introduce an anti-resonance frequency at about 39 and 26 Hz, respectively. The resonance peak due to the primary mass is also visible at around 22 Hz, as well as the second resonance peak introduced by the neutralizer at about 40 and 30 Hz, respectively.

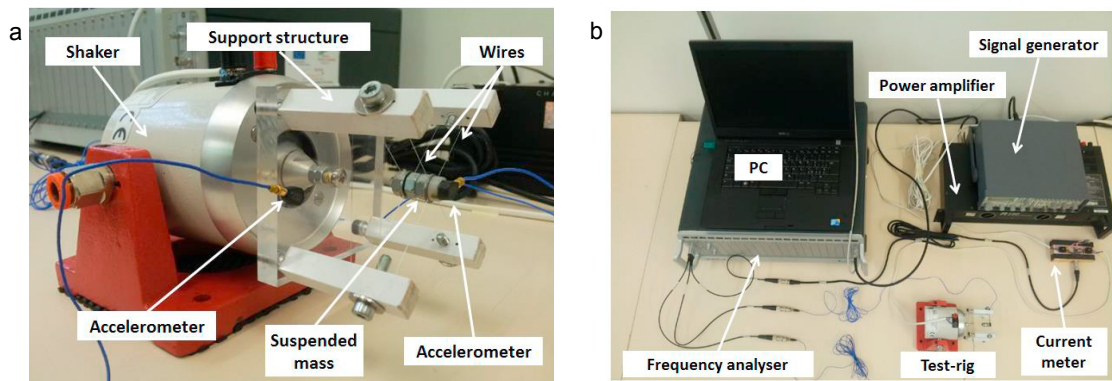


Fig. 1. Photograph of (a) the test-rig used in the experiments, and (b) the experimental setup.

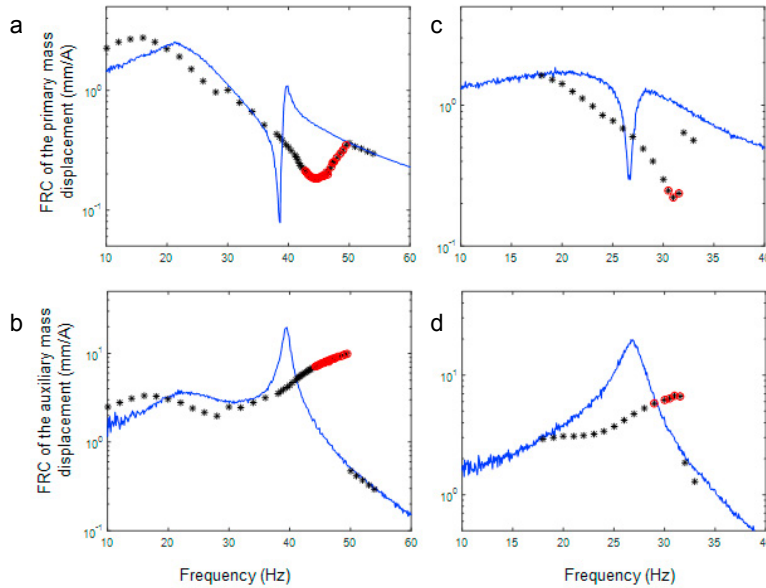


Fig. 2. Experimental FRCs of the system in case of tighter (a)-(b) and looser (c)-(d) wires. Results for the primary mass are shown in (a) and (c); results for the auxiliary mass are shown in (b) and (d). Blue solid lines correspond to the low-level white noise excitation. Black star markers correspond to harmonic excitation response in case of high-amplitude excitation. The red circles denote cases where response was not harmonic.

In a second phase, the shaker was supplied with a sinusoidal input signal at each frequency. The amplitude of the supplied voltage was manually adjusted to guarantee a constant current (0.4 A) flowing into the shaker coil, and this was measured by the meter indicated in Fig. 1(b). For the two masses, acceleration time-histories were measured by the accelerometers, and the corresponding spectrum was estimated by the frequency analyser. The amplitude at the excitation frequency is then plotted in Fig. 2(a)-(d) with a black star marker. It was checked that the system response was predominantly harmonic, and the cases where other harmonics with an amplitude greater than 10% of that at the excitation frequency were present, have been indicated by a red circle.

It can be seen that the increase in the amplitude of excitation has a profound effect on the shape of the FRC, and this is typical of nonlinear systems [6]. In particular, the response of the primary oscillator, in Fig. 2(a) and (c), is characterized by a shift of the anti-resonance frequency to the higher frequencies. While the response of the auxiliary oscillator, i.e. the neutralizer, in Fig. 2(b) and (d), is characterized by a bending of the resonance peak to the higher frequencies, which then reveals a jump-down [7] at about 50 and 32 Hz, respectively.

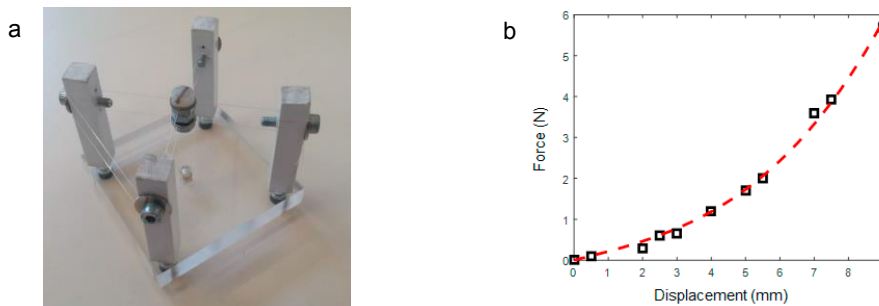


Fig. 3. (a) Photograph of the neutralizer alone. (b) Experimentally estimated force-deflection curve (black markers), and cubic polynomial fitting (red dashed line).

To get some clear evidence of the presence of nonlinearity into the system, the static force-deflection curve of the neutralizer was experimentally determined. To this purpose, the neutralizer with its support structure was disassembled from the shaker and set on an horizontal surface, as illustrated in Fig. 3(a). Weights of known mass were positioned onto the neutralizer mass, and the corresponding deflection due to gravity was measured. Each pair of measurements is plotted in Fig. 3(b), as a black square marker. It is then speculated [8] that the force-deflection curve of the neutralizer under investigation is of cubic type, and a polynomial curve with linear and cubic coefficients is then fitted to the experimental data. The result is shown in Fig. 3(b) as a red dashed line. This is believed to be the main source of nonlinearity into the system.

3. Model of the system

Based on the experimental observation reported above, the test-rig illustrated in Fig. 1(a) is modelled as shown in Fig. 4, where the shaker is modelled as a linear mass-damper-spring system excited by an harmonic force of amplitude F and angular frequency ω in time t . The corresponding mass, damping coefficient and stiffness are denoted by m_s , c_s and k_s , respectively. An auxiliary oscillator of mass m is attached to the primary mass through a suspension with damping coefficient c_1 and nonlinear stiffness with linear, k_1 , and cubic, k_3 , coefficients.

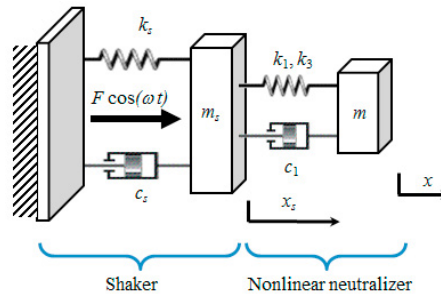


Fig. 4. Model of the system under study.

The equations of motion of the two degrees of freedom system shown in Fig. 4 are

$$\begin{aligned}
 m_s \ddot{x}_s + c_s \dot{x}_s + k_s x_s + c_1 \dot{z} + k_1 z + k_3 z^3 &= F \cos(\omega t) \\
 m \ddot{x} - m \ddot{z} - c_1 \dot{z} - k_1 z - k_3 z^3 &= 0
 \end{aligned}
 \tag{1a,b}$$

where x_s and x are the displacements of the primary and auxiliary mass, respectively, while $z = x_s - x$ is the relative displacement. It is assumed that the force amplitude is proportional to the current supplied to the shaker.

A non-dimensional form of the solutions to Eqs. (1a,b) in terms of amplitude-frequency equations, is reported from [9,10] in Appendix A, and is used to plot the FRC in Fig. 5(a)-(f), for the values of parameters listed in Table 1. They correspond approximately to those of the experimental rig in Fig. 1(a). Also, the values for k_1 and k_3 , in the first line of Table 1, correspond to those of the cubic force-deflection curve plotted in Fig. 3(b).

It is worth noting that the model in [9] overcomes some limitations for the values of the mass of the neutralizer relative to the mass of the primary system, which were present in [11].

Table 1. System parameters used to plot Fig. 5(a)-(d).

Figures	m_s [kg]	k_s [N/m]	c_s [Ns/m]	m [kg]	c_1 [Ns/m]	k_1 [N/m]	k_3 [N/m ³]	F [N]
(a)-(b)	0.13	3500	20	0.005	0.01	210	5×10^6	2
(c)-(d)	0.13	3500	20	0.005	0.01	310	1×10^7	2
(e)-(f)	0.13	3500	0.5	0.006	0.02	150	1×10^5	2

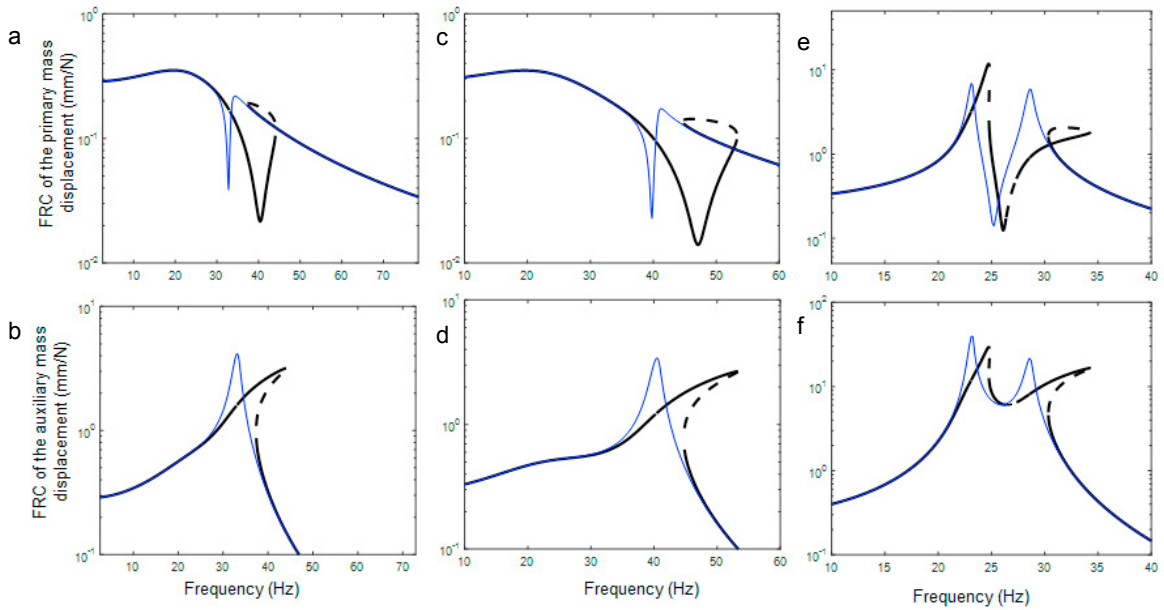


Fig. 5. Analytical FRCs of the coupled system for the values of parameters listed in Table 1. Blue thin solid lines correspond to the linear case, where $F = 0.2$ N. Black thick solid (dashed) lines correspond to the stable (unstable) solutions for $F = 2$ N.

It can be seen that the theoretical solution to the model reported in Fig. 4 captures qualitatively the behavior of the experimental test-rig. In particular, it can be noted that in the case of low-amplitude excitation ($F = 0.2$ N), the system behaves in a linear fashion (blue thin solid lines). When $F = 2$ N, however, the nonlinearity is excited and this changes the shape of the FRCs as shown by the black thick lines. The qualitative behavior is in agreement with the experimental results reported in Fig. 2. Also, Fig. 5(e) and (f) report evidence of instabilities around the anti-resonance, as observed in the experiments. It is believed that the use of a proper parameter identification technique, as a next step, will allow a more quantitative comparison.

4. Conclusions

This paper has presented a preliminary investigation on the effect of a nonlinear neutralizer to control the vibration of a linear oscillator. Based on phenomena observed in experiments, a model of the system is proposed which qualitatively captures its fundamental characteristics. It is shown how the introduction of a nonlinear stiffness in the neutralizer suspension has the effect of shifting the anti-resonance frequency to the higher frequencies, and increase the bandwidth of the device around the anti-resonance, for fixed level of damping. Potentially, nonlinearity could then be used instead of damping to improve the robustness of the device to mistuning. A disadvantage that may arise is due to the appearance of instability regions around the anti-resonance frequency, which could lead to higher vibration levels due to the presence of lower and higher order harmonics. This motivates further investigation, as well as the challenge to adjust the neutralizer suspension stiffness (i.e. the wire tension) using adaptive control.

Appendix A. Non-dimensional amplitude-frequency equations

The non-dimensional solutions to the equations of motion in Eqs. (1a,b) are reported from [9] as

$$Y_s^2 = \frac{1 - W^4 \left[-\frac{3}{2} \mu (1 - \Omega^2 (1 + \mu)) \right] - W^2 \left[\Omega^4 \mu^2 - 2\mu (1 - \Omega^2 (1 + \mu)) (\Omega_0^2 - \Omega^2) + 8\zeta_s \zeta_s \mu \Omega^2 \right]}{(1 - \Omega^2 (1 + \mu))^2 + 4\zeta_s^2 \Omega^2}$$

$$\begin{aligned}
 Y^2 &= (Y_s \cos(\varphi_s) - W \cos(\varphi))^2 + (Y_s \sin(\varphi_s) - W \sin(\varphi))^2 \\
 \frac{9}{16} \gamma^2 W^6 &+ \left[\frac{3}{2} (\Omega_0^2 - \Omega^2) + \Omega^4 \frac{-\frac{3}{2} \mu (1 - \Omega^2 (1 + \mu))}{(1 - \Omega^2 (1 + \mu))^2 + 4 \zeta_s^2 \Omega^2} \right] \gamma W^4 + \left[-\frac{\Omega^4}{(1 - \Omega^2 (1 + \mu))^2 + 4 \zeta_s^2 \Omega^2} \right] + \dots \\
 \left[\frac{(\Omega_0^2 - \Omega^2)^2 + 4 \zeta_s^2 \Omega^2 + \Omega^4 \frac{\Omega^4 \mu^2 - 2 \mu (1 - \Omega^2 (1 + \mu)) (\Omega_0^2 - \Omega^2) + 8 \zeta \zeta_s \mu \Omega^2}{(1 - \Omega^2 (1 + \mu))^2 + 4 \zeta_s^2 \Omega^2}}{(1 - \Omega^2 (1 + \mu))^2 + 4 \zeta_s^2 \Omega^2} \right] W^2 &= 0
 \end{aligned}$$

where the mass ratio μ , damping ratios ζ_s and ζ , frequency ratio Ω_0 , nonlinearity γ and non-dimensional frequency of excitation Ω are defined, respectively, as

$$\mu = m/m_s, \zeta_s = c_s/2\sqrt{m_s k_s}, \zeta = c_1/2\mu\sqrt{m_s k_s}, \Omega_0 = \sqrt{k_1/\mu k_s}, \gamma = k_3 F^2 / \mu k_s^3, \Omega = \omega/\omega_s$$

Y_s , Y and W are the amplitudes of the non-dimensional displacements of the two masses and the relative displacement between them, which are given, respectively, as

$$y_s = x_s k_s / F, y = x k_s / F, w = z k_s / F$$

and φ_s , φ are, respectively, the phases of the non-dimensional displacements of the two masses, and are given by

$$\begin{aligned}
 \varphi_s &= \arctan \left(\frac{-2 \zeta_s \Omega Y_s - \Omega \mu \frac{2 \zeta W^2}{Y_s}}{Y_s (1 - \Omega^2 (1 + \mu)) - \mu \frac{W^2}{Y_s} \left(\Omega_0^2 - \Omega^2 + \frac{3}{4} \gamma W^2 \right)} \right) \\
 \varphi &= \arctan \left(\frac{\frac{-W}{\Omega^2 Y_s} \left(\Omega_0^2 - \Omega^2 + \frac{3}{4} \gamma W^2 \right) \sin(\varphi_s) - \frac{-2 \zeta W}{\Omega Y_s} \cos(\varphi_s)}{\frac{-W}{\Omega^2 Y_s} \left(\Omega_0^2 - \Omega^2 + \frac{3}{4} \gamma W^2 \right) \cos(\varphi_s) + \frac{-2 \zeta W}{\Omega Y_s} \sin(\varphi_s)} \right)
 \end{aligned}$$

References

[1] H. Frahm, Device for damping vibrations of bodies, US Patent No. 989, 958 (1911).
 [2] J. Ormondroyd, J.P. Den Hartog, Theory of the dynamic absorber, Transactions of the ASME, APM 50 (1928) 11–22.
 [3] P.L. Walsh, J.S. Lamancusa, A variable stiffness vibration absorber for the minimization of transient vibrations, J Sound Vib 158 (1992) 195–211.
 [4] P. Bonello, M.J. Brennan, S.J. Elliott, Vibration control using an adaptive tuned vibration absorber with a variable curvature stiffness element, Smart Mater Struct 14 (2005) 1055–1065.
 [5] M.J. Brennan, Characteristics of a wideband vibration neutralizer, Noise Control Eng J 45 (1997) 201–207.
 [6] A.H. Nayfeh, D.T. Mook, Nonlinear Oscillations, Wiley, New York, 1979.
 [7] K. Worden, On jump frequencies in the response of the Duffing oscillator, J Sound Vib 198 (1996) 522–525.
 [8] M.J. Brennan, G. Gatti, The characteristics of a nonlinear vibration neutralizer, J Sound Vib 331 (2012) 3158–3171.
 [9] G. Gatti, Uncovering inner detached resonance curves in coupled oscillators with nonlinearity, J Sound Vib 372 (2016) 239–254.
 [10] G. Gatti, M.J. Brennan, Inner detached frequency response curves: an experimental study, J Sound Vib 396 (2017) 246–254.
 [11] G. Gatti, M.J. Brennan, On the effects of system parameters on the response of a harmonically excited system consisting of weakly coupled nonlinear and linear oscillators. Journal of Sound and Vibration 330 (2011) 4538–4550.